

# Decision Making in Cryptocurrency-Backed Loans: A Volatility and Liquidity Integrated Approach

Si Yuan Jin<sup>1,2</sup>, Bing Zhu<sup>\*2</sup>, Zi Yuan Li<sup>\*2</sup>, and Yong Xia<sup>\*2</sup>

<sup>1</sup>School of Business and Management, Hong Kong University of Science and Technology

<sup>2</sup>HSBC Lab, HSBC Holdings plc, Guangzhou, China

This version: December 17, 2023

## Abstract

Cryptocurrencies are disrupting traditional banking through the rising demand for cryptocurrency-based financial services. However, uncertainty deters traditional institutions from offering such services, as the risks associated with cryptocurrency-backed loans remain unclear. We present a procedure to secure cryptocurrency-backed loans, including calculating loan-to-value, margin call, and liquidation ratios. Our value-at-risk (VaR) model accounts for both volatility and liquidity risks. Our value-at-risk (VaR) model accounts for volatility and liquidity risks. We estimate volatility VaR using a generalized autoregressive conditionally heteroskedastic (GARCH) model and test six distributions to find the best fit based on return residuals. We calculate liquidity risk using the bid-ask spread (BAS) from transaction data and a GARCH-like model to extract BAS variance, then derive liquidity-adjusted VaR. Combining the two VaRs gives ratios for different periods. To validate our method, we statistically analyzed the entire cryptocurrency market and backtested using data from two recent crashes. Our findings offer implications for financial institutions, regulators, and cryptocurrency platforms to better manage risks of cryptocurrency services.

**Keywords:** cryptocurrency-backed loans, volatility risk, liquidity risk

---

\*Corresponding Authors: bingl.zhu@hsbc.com, stan.ziyuan.li@hsbc.com.cn, yong.xia@hsbc.com

# 1 Introduction

Web 3.0 services are predicted to reach a market size of \$88 trillion by 2030 [1], which has prompted traditional financial institutions to explore the benefits of incorporating cryptocurrency into their business models, such as cryptocurrency-backed loans. Similar to other collateral loans [2], cryptocurrency-backed loans provide liquidity to clients while allowing them to retain cryptocurrency ownership. On the other hand, the assignment of collateral provides an incentive for the borrower to repay the loan [3]. Several platforms, including SALT Lending, Crypto.com, Celsius Network, BlockFi, Nexo, YouHODLER, Inlock, CoinLoan, Dharma, have offered cryptocurrency-backed loans (Table 1) with different loan-to-value (LTV) ratio (40-90%) and annual percentage rate (APR), indicating lack of robust mechanisms that underpin these figures. Despite the growing demand of these services, the literature lacks a robust cryptocurrency-backed loan mechanism design, which deters traditional financial institutions from the service. Our study aims to provide a theoretical cryptocurrency-backed loan evaluation with empirical verification.

Table 1: Survey of Collateral Loan of BTC, Collected in May 2022.

Platform	LTV (%)	Warning(%)	Liquidation(%)	APR (%)
Coinbase	40	60	85	8
Lendingblock	50	65	-	6.4 - 10
Celsius Network	50	65	80	8.95
Ledn	50	70	80	7.9
BlockFi	50	70	80	9.75
Crypto.com	50	70	90	12
Nexo	50	71.4	83.3	5.9 - 11.9
LendaBit	50	85	95	8
Binance	65	75	83	9
OKX	70	80	92	2.5 - 5
CoinLoan	70	80	90	7.5
Helio	75	-	-	9
YouHODLER	90	94.7	97.6	15.20 - 20.68
Inlock	90	-	-	13.7

When dealing with volatile assets, including stocks [4] and real estates [5], lenders typically consider volatility risk, liquidity risk, and credit risk. Volatility risk refers to the potential reduction or default in collateral value, escalating the lender's loan exposure. Liquidity risk involves the costs arising during the liquidation of collateral in response to borrower default or collateral value drop [6]. Credit risk symbolizes the potential losses to lenders when borrowers default, a risk inherently connected to both volatility and liquidity risks [7]. Lenders often use the LTV ratio, a risk evaluation measure, to compare the loan amount to the collateral value, while warning and liquidation ratios can mitigate credit risk. If the pledged cryptocurrencies' value decreases to the warning

ratio, borrowers are advised to add more collateral. If the cryptocurrency value further declines to the liquidation ratio, the collateral is liquidated by lenders to secure the loan. Our study focuses on the volatility and liquidity risks associated with cryptocurrency-based loans, leaving credit risk analysis for future research, as credit risk analysis depends on the characteristics of borrowers. Our analysis assumes borrowers are lowest-risk where collateral is required for each loan [2].

The VaR model, widely employed to quantify volatility risk, calculates potential losses during a specified time horizon due to fluctuating asset prices at a given confidence level [8]. Determining VaR requires the asset volatility from the loss (or return) probability distribution function (PDF). Various methods have been developed for obtaining the PDFs, including Monte Carlo simulations based on stochastic processes [9], the GARCH model [10], historical simulation [11], rule-based checking [12]. Loan processing is a complex process requiring comparisons of diverse models [4, 13, 14]. We test and compare various assumptions for the return distribution in the standard GARCH model, particularly mixed distributions with multiple components [15]. Our findings suggest that mixed Gaussian and T or Skew T distributions typically yield the best performance in characterizing cryptocurrency volatility, which may plausibly indicate the distinct behaviors of heterogeneous groups of market players [16].

Liquidity risk comprises both market and internal factors [6]; the former refers to the ease with which an asset can be bought or sold in the market, while the latter pertains to the time required for an institution to liquidate collateral. Our model considers only market liquidity risk and incorporates it into the VaR calculation by employing a liquidity-adjusted VaR [17] to thoroughly evaluate the LTV ratio. Furthermore, we construct a GARCH-like model to facilitate a dynamic and predictive representation of the liquidity VaR, calculated as the BAS [18] from transaction-based data. By combining the accurately determined volatility and liquidity risks, we can compute the LTV, warning, and liquidation ratios for cryptocurrency-pledged loans.

Our contributions to the literature on cryptocurrency-backed loan services are three-fold. Firstly, we contribute to the information system literature by developing a comprehensive theoretical procedure for cryptocurrency-backed financial services. The literature has studied cryptocurrency price [19, 20], exchange rate [21], ICO designs [22, 23, 24], and token-based platform [25]. Little is known about cryptocurrency-backed loan services. Answering the call for building powerful decision support tools, We present a general procedure for calculating LTV ratios based on the VaR model for all available cryptocurrencies, encompassing both volatility and liquidity VaR. The empirical validation results prove the utility of the model. Our empirical investigation compares estimates from two consecutive periods, which generates insights into the institution's decision-making in emerging financial markets by revealing the phasing out of market dynamics and the emerging significance of technology factors in driving the fundamental value of cryptocurrencies.

Secondly, financial instrument risk assessment has always been an important area in decision support research [26, 27, 28, 29, 30], and there has been continuous interest in financial service management. Results from our research contribute to our understanding of the cryptocurrency risk dynamics, providing important managerial insights in enabling more efficient, data-driven risk decision-making.

Our work has practical implications for traditional financial institutions to provide cryptocurrency-backed loan services and subsequent cryptocurrency services [31]. While loan processing literature has studied collateral loans in the traditional financial market [3, 4, 13, 14, 32], little is known about cryptocurrency-backed loans. Our model can provide traditional institutions with a robust mechanism for determining the loan-to-value, warning, and liquidation ratio for cryptocurrency-backed loans. Given the rapid development of technology and growing market recognition, the cryptocurrency market could cause disruptive changes in the financial industry, making it critical to build up a solid theoretical foundation for future practices.

## 2 Data Description

The daily price data for cryptocurrencies employed in this study are sourced from CoinMarketCap, a comprehensive resource providing daily values for over 19,000 cryptocurrencies. The data points include the opening (00:00:00 UST), high, low, and closing (24:00:00 UST) prices, the 24-hour trading volume, and the total market capitalization. Our analysis focuses on the top 3,000 cryptocurrencies ranked by market capitalization, excluding stablecoins such as USDT, USDC, DAI, and the like.

For different sections of our paper, we select varied quantities of cryptocurrencies to serve specific analytical purposes. To illustrate our methodologies, we select three representative coins: BTC, ETH, and MANA. BTC is the world’s first cryptocurrency, and ETH is renowned for its utilization of smart contracts that implement a Turing-complete blockchain network. MANA is the cryptocurrency associated with Decentraland, a decentralized virtual world platform whose software is based on the Ethereum blockchain, enabling users to create, experience, and monetize content. For the sections presenting a statistical analysis of results, we will incorporate data from approximately 3,000 cryptocurrencies. We present our final results on LTV, warning, and liquidation ratios, along with the corresponding back-testing results, by selecting the top 10 cryptocurrencies by market capitalization.

We use the natural logarithm form in calculating cryptocurrency returns,  $r_t = \log(C_t/C_{t-1})$ , where  $C_t$  is the closing price. An example of the data for BTC spanning from April 28, 2013, to May 15, 2022, with 3,305 data points, is demonstrated in Fig. 1. The daily closing price  $C_t$  and return

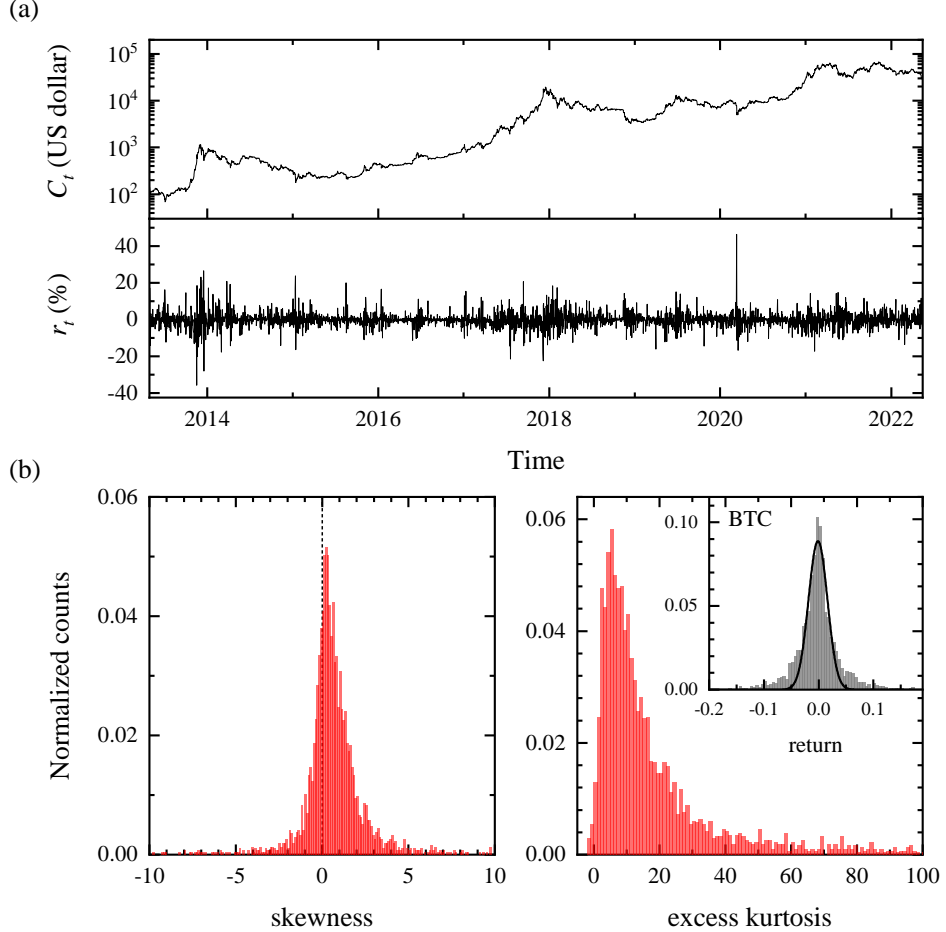


Figure 1: (a) Daily Price and Return of BTC. (b) Skewness and Excess Kurtosis Distribution of the Top 3,000 Cryptocurrencies. The inset portrays the return distribution of the BTC coin, which exhibits a skewness of approximately  $-0.52$  and an excess kurtosis of  $\approx 11$ . The distribution is conspicuously asymmetrical, and a Gaussian fit (denoted by the black curve) to the data is conducted to highlight the fat-tail effect.

$r_t$  are plotted at the top and bottom of Fig. 1 (a), respectively. From the return data obtained, we calculate certain statistical properties such as the mean ( $\mu$ ) and the  $i$ th central moment  $m_i$ , which are defined as

$$\begin{aligned} \mu &= \frac{1}{N} \sum_{t=1}^N r_t, \\ m_i &= \frac{1}{N} \sum_{t=1}^N (r_t - \mu)^i. \end{aligned} \tag{1}$$

The skewness and excess kurtosis of the dataset are computed as  $m_3/m_2^{3/2}$  and  $m_4/m_2^2 - 3$ , respectively. Their distributions for the top 3,000 cryptocurrencies with the largest market capitalization are plotted in Fig. 1 (b). A non-zero skewness suggests an asymmetric distribution of returns,

which is often observed in many cryptocurrencies. Kurtosis measures whether the data are heavy-tailed or light-tailed relative to a normal distribution. The BTC coin serves as a prime example, as shown in the inset of Fig. 1 (b), where the return distribution is asymmetric and showcases the well-documented fat-tail effect [33]. This is corroborated by its skewness ( $\approx -0.52$ ) and excess kurtosis ( $\approx 11$ ) values.

## 3 Methodology

### 3.1 Background

In accordance with the established literature [31], the daily LTV ratio, denoted as  $\eta_t$ , can be formulated as follows:

$$\eta_t = 1 - \text{VaR}_t^V - \text{VaR}_t^L, \quad (2)$$

where  $\text{VaR}_t^V$  and  $\text{VaR}_t^L$  represent the volatility and liquidity VaR, respectively.

The volatility VaR,  $\text{VaR}_t^V$ , is inherently associated with the return distribution:

$$\text{VaR}_t^V = 1 - e^{F^{-1}(k)}, \quad (3)$$

where  $F^{-1}(k)$  refers to the inverse function of the return cumulative distribution function (CDF)  $F(y)$  with a confidence level of  $1 - k$ . The integral of its PDF  $f(x)$ ,  $F(y) = \int_{-\infty}^y f(x)dx$ , determines  $F(y)$ . Parameters characterizing  $f(x)$  can be obtained through models such as the GARCH model. The GARCH model can capture critical characteristics of financial time series, such as time-varying heteroskedasticity and volatility clustering [34].

The inclusion of  $\text{VaR}^L$  in the LTV calculation, as expressed in Eq. (2), is crucial due to liquidity risks. A vital metric to quantify market liquidity risk is the BAS [18], which signifies the difference between bid and ask prices in the market. The daily BAS, denoted as  $\text{BAS}_t$ , allows us to compute  $\text{VaR}^L$  as follows:

$$\text{VaR}_t^L = \frac{1}{2} F_{\text{BAS}}^{-1}(1 - k). \quad (4)$$

Similar to Eq. (3),  $F^{-1}\text{BAS}(1 - k)$  is the inverse function of the CDF,  $F_{\text{BAS}}(y)$ , of the BAS distribution, and  $k$  represents the confidence level. Thus, a significant proportion of the liquidity cost is covered here (99% if  $k = 0.01$ ). According to Ref. [35], the  $\text{BAS}_t$  distribution follows a lognormal PDF, which can be expressed as:

$$f_{\text{BAS}}(x) = \frac{1}{\sqrt{2\pi}x\sigma} e^{-\frac{(\ln x - \mu)^2}{2\sigma^2}}, \quad (5)$$

with the parameters  $\mu$  and  $\sigma$  representing the mean and variance of a normal distribution, respectively. This assumption has been empirically verified in the context of cryptocurrency BAS distribution [36]. With the lognormal PDF as shown in Eq. (5), the liquidity VaR,  $\text{VaR}_t^L$ , as formulated in Eq. (4), can be redefined as:

$$\text{VaR}_t^L = \frac{1}{2} \exp[\mu + \sqrt{2}\sigma\text{Erf}^{-1}(1 - 2k)], \quad (6)$$

where  $\text{Erf}^{-1}(x)$  represents the inverse error function.

This comprehensive formulation provides a robust foundation for understanding the calculation of LTV ratios, incorporating both volatility and liquidity risks. The procedures presented offer a sophisticated approach to measuring risk and value within the cryptocurrency market, contributing significantly to the extant body of knowledge in the field.

## 3.2 GARCH Model

The GARCH model, extended from the ARCH model [10], has been widely employed to analyze the volatility. GARCH model assumes that the residual return  $\epsilon_t = r_t - \mu$  adheres to a specific PDF with zero mean and a variance  $\sigma_t^2$ . This PDF could be a Gaussian, Student's T, or Skewed T distribution [37]. The standard GARCH( $p, q$ ) model is given by Equation 7:

$$\begin{aligned} r_t &= \mu + \epsilon_t, \\ \sigma_t^2 &= \omega + \sum_{i=1}^q \alpha_i \epsilon_{t-i}^2 + \sum_{i=1}^p \beta_i \sigma_{t-i}^2. \end{aligned} \quad (7)$$

where  $(q, p)$  denotes the number of auto-correlation terms.  $\omega \geq 0$  is a constant,  $\alpha_i > 0$  are known as Arch parameters, and  $\beta_i \geq 0$  are designated as GARCH parameters. In the context of this paper, we focus primarily on a  $(q, p) = (1, 1)$  model for simplicity, denoting  $\alpha_1 \equiv \alpha$  and  $\beta_1 \equiv \beta$ . The model parameters  $\mu$ ,  $\omega$ ,  $\alpha$ , and  $\beta$  are estimated from historical return data, often using the Maximum Likelihood Estimation (MLE) method [38]. Once these parameters are established, the GARCH model can be utilized to predict future volatility, and subsequently to calculate the  $L$ -th percentile VaR ( $\text{VaR}_t^L$ ).

### 3.2.1 The Residual Distribution

In the study of cryptocurrency volatility, numerous GARCH-type models have been proposed, featuring a variety of regression formulas and residual distributions [39, 40]. As indicated by Fig. 1 (b), the return distribution of many cryptocurrencies is heavily fat-tailed and asymmetric. This observation necessitates the use of non-normal, asymmetric distribution functions for cryptocurrency residuals, such as Skewed T and Skewed GED distributions [40].

One alternative approach to describing asymmetric, fat-tailed residual distributions in GARCH models is to assume mixed distributions [15]. This means the PDF is a mixture of different distributions, an idea originally proposed in [41]. A GARCH model utilizing a mixed distribution can not only capture key stylized facts such as volatility clustering, heavy tails, time-varying skewness, and the leverage effect, but it may also offer insights into the behavior of heterogeneous market player groups [16].

A general PDF  $f(x)$  that is a mixture of  $n$  independent distributions can be expressed as:

$$f(x) = \sum_{i=1}^n \rho_i f_i(x; \mu_i, \sigma_i^2), \quad (8)$$

where  $f_i(x; \mu_i, \sigma_i^2)$  represents the  $i$ -th component, normalized such that  $\int_{-\infty}^{+\infty} f_i(x; \mu_i, \sigma_i^2) dx = 1$ , with mean  $\mu_i$  and variance  $\sigma_i^2$ . The weights,  $\rho_i$ , satisfy  $\sum_{i=1}^n \rho_i = 1$  and  $0 \leq \rho_i \leq 1$ . The mean and variance of  $f(x)$  are given by:

$$\begin{aligned} \mu &= \int_{-\infty}^{+\infty} x f(x) dx = \sum_{i=1}^n \rho_i \mu_i, \\ \sigma^2 &= \int_{-\infty}^{+\infty} (x - \mu)^2 f(x) dx = \sum_{i=1}^n \rho_i \sigma_i^2 + \sum_{i=1}^n \rho_i (\mu_i - \mu)^2. \end{aligned} \quad (9)$$

Within this PDF framework, the GARCH model (7) is modified to:

$$\begin{aligned} r_t &= \mu + \epsilon_t, \\ \vec{\sigma}_t^2 &= \omega + \vec{\alpha} \epsilon_{t-1}^2 + \beta \vec{\sigma}_{t-1}^2, \end{aligned} \quad (10)$$

where  $\vec{\sigma}_t = (\sigma_{1,t}, \sigma_{2,t}, \dots, \sigma_{n,t})^T$  denotes the  $n$  variances,  $\vec{\alpha} = (\alpha_1, \alpha_2, \dots, \alpha_n)^T$  with  $\alpha_i \in [0, 1]$ ,  $\beta$  is a  $n \times n$  matrix in general, and we assume that a common  $\omega$  is shared among  $\sigma_{i,t}$  ( $i = 1, 2, \dots, n$ ). We confine our study to the case where  $\beta$  is a diagonal matrix, i.e.  $\beta = \text{diag}(\beta_1, \beta_2, \dots, \beta_n)$ . The persistency of the model can be ensured by the following constraint: The largest eigenvalue of the matrix  $\vec{\alpha} \vec{\rho} + \beta$ , denoted as  $\kappa_{\max}$ , is less than or equal to 1, where  $\vec{\rho} = (\rho_1, \rho_2, \dots, \rho_n)$ .

We consider six distinct distributions with a maximum of two components: the Gaussian, T, Skewed T, double-Gaussian (DG), mixed T and Gaussian (MTG), and mixed Skewed T and Gaussian (MSG) distributions. The exact functional forms of these distributions are defined in the subsequent section. Additionally, their corresponding cumulative distribution functions (CDFs) are included to facilitate the computation of VaR using Eq. (3).

**a. Gaussian distribution** The PDF and CDF of a Gaussian distribution:

$$f_G(x, \mu, \sigma) = \frac{1}{\sigma\sqrt{2\pi}} \exp\left(-\frac{1}{2}\left(\frac{x-\mu}{\sigma}\right)^2\right),$$

$$F_G(x, \mu, \sigma) = \frac{1}{2}\left[1 + \text{Erf}\left(\frac{x-\mu}{\sqrt{2}\sigma}\right)\right],$$
(11)

where  $\mu$  and  $\sigma^2$  represent the mean and variance, respectively.

**b. T distribution** The T distribution is described by the following PDF and CDF:

$$f_T(x, \mu, \sigma, \nu) = \frac{\Gamma\left(\frac{\nu+1}{2}\right)}{\sigma\sqrt{(\nu-2)\pi}\Gamma\left(\frac{\nu}{2}\right)} \left[1 + \frac{1}{\nu-2}\left(\frac{x-\mu}{\sigma}\right)^2\right]^{-\frac{(\nu+1)}{2}},$$

$$F_T(x, \mu, \sigma, \nu) = F_0(m, \nu) = \frac{1}{2} + \frac{m\Gamma\left(\frac{\nu+1}{2}\right)}{\sqrt{(\nu-2)\pi}\Gamma\left(\frac{\nu}{2}\right)} {}_2F_1\left(\frac{1}{2}, \frac{\nu+1}{2}, \frac{3}{2}, -\frac{m^2}{\nu-2}\right),$$
(12)

where  $m = (x-\mu)/\sigma$ ,  $\mu$  represents the mean,  $\sigma^2$  is the variance,  $\nu > 2$  is the number of degrees of freedom (DOF),  $\Gamma(y)$  is the Gamma function, and  ${}_2F_1$  represents the hypergeometric function.

**c. Skewed T distribution** The PDF and CDF of a Skewed T distribution:

$$f_{ST}(x, \mu, \sigma, \nu, \lambda) = \frac{bc}{\sigma}[1 + \frac{1}{\nu-2}(\frac{a+b(x-\mu)/\sigma}{1+\text{sgn}((x-\mu)/\sigma+a/b)\lambda})^2]^{-(\nu+1)/2},$$

$$F_{ST}(x, \mu, \sigma, \nu, \lambda) = [1 + \text{sgn}(m)\lambda]F_0(\frac{m}{1+\text{sgn}(m)\lambda}, \nu) - H(m)\lambda.$$
(13)

where  $a = 4\lambda c \frac{\nu-2}{\nu-1}$ ,  $b^2 = 1 + 3\lambda^2 - a^2$ ,  $c = \frac{\Gamma(\frac{\nu+1}{2})}{\sqrt{\pi(\nu-2)\Gamma(\frac{\nu}{2})}}$ ,  $m = a + b(x-\mu)/\sigma$ ,  $\text{sgn}(m)$  and  $H(m)$  are the Sign and Heaviside function of  $m$ , respectively, and the function  $F_0$  is defined in Eq. (12). The parameters  $\mu$ ,  $\sigma^2$  and  $\nu > 2$  are analogous to those in the T distribution, while  $-1 < \lambda < 1$  modulates the degree of asymmetry, i.e.,  $\lambda = 0$  results in the symmetric T distribution.

**d. Double-Gaussian distribution** The DG distribution is characterized by the subsequent PDF and CDF:

$$f_{DG}(x) = (1-\rho)f_G(x, \mu_1, \sigma_1) + \rho f_G(x, \mu_2, \sigma_2),$$

$$F_{DG}(x) = (1-\rho)F_G(x, \mu_1, \sigma_1) + \rho F_G(x, \mu_2, \sigma_2),$$
(14)

Here,  $0 < \rho < 1$  symbolizes the weight of the second Gaussian.

**e. Mixed T and Gaussian distribution** The MTG distribution is described by the following PDF and CDF:

$$f_{MTG}(x) = (1-\rho)f_G(x, \mu_1, \sigma_1) + \rho f_T(x, \mu_2, \sigma_2, \nu),$$

$$F_{MTG}(x) = (1-\rho)F_G(x, \mu_1, \sigma_1) + \rho F_T(x, \mu_2, \sigma_2, \nu).$$
(15)

Similar to the DG distribution,  $\rho$  denotes the weight of the T distribution.

**f. Mixed Skew T and Gaussian distribution** The PDF and CDF of an MSG distribution are represented as:

$$\begin{aligned} f_{MSG}(x) &= (1 - \rho)f_G(x, \mu_1, \sigma_1) + \rho f_{ST}(x, \mu_2, \sigma_2, \nu, \lambda), \\ F_{MSG}(x) &= (1 - \rho)F_G(x, \mu_1, \sigma_1) + \rho F_{ST}(x, \mu_2, \sigma_2, \nu, \lambda), \end{aligned} \quad (16)$$

In this context,  $\rho$  represents the weight of the Skew T distribution.

The presented mathematical representations form the basis for understanding the different forms of distribution, their characteristics, and the influence of their parameters. The Gaussian distribution, T distribution, Skewed T distribution, DG distribution, MTG, and MSG distribution all have distinct attributes that make them suitable for modeling a variety of data distributions. Each distribution is defined by a specific set of parameters that determine its shape, center, and spread.

The Gaussian distribution, defined by the mean and variance, is the most commonly used due to its simplicity and the central limit theorem. The T distribution, with an additional degree of freedom parameter, provides a more flexible model, particularly for data with heavier tails. The Skewed T distribution extends this even further by allowing for asymmetry. DG and Mixed distributions incorporate a weight parameter, which allows for modeling data that show a combination of two different distributions. This can be particularly useful for data with multiple modes or different behaviors in different ranges.

This examination of different distribution types is crucial for understanding the nature of residuals in data analysis, and selecting the most appropriate distribution can significantly impact the reliability and interpretability of results.

### 3.2.2 Estimating Parameters of GARCH Model with Various Distributions

We have a set of  $n$  independent observations, denoted by  $\vec{x} = (x_1, x_2, \dots, x_n)$ , that conform to an identical underlying distribution  $f(x; \vec{\theta})$ . Here,  $\vec{\theta}$  represents the set of parameters. The likelihood for the observed values  $\vec{x}$  can be expressed as:

$$L(\vec{x}; \vec{\theta}) = \arg \max_{\vec{\theta}} \prod_{t=1}^n \{f(x_t; \vec{\theta})\}. \quad (17)$$

The MLE of the parameters corresponds to the values of  $\vec{\theta}$  that maximize  $L(\vec{x}; \vec{\theta})$ . In essence, the fitted parameters present the highest probability of representing the observed data.

For a given return  $r_t$ , we use the GARCH model based on various PDFs specified in Section 3.2.1 for the distribution of the residual  $\epsilon_t$ . To compare different distributions for the GARCH model, we adopt three distinct criteria: Akaike Information Criteria (AIC), Bayesian Information Criterion

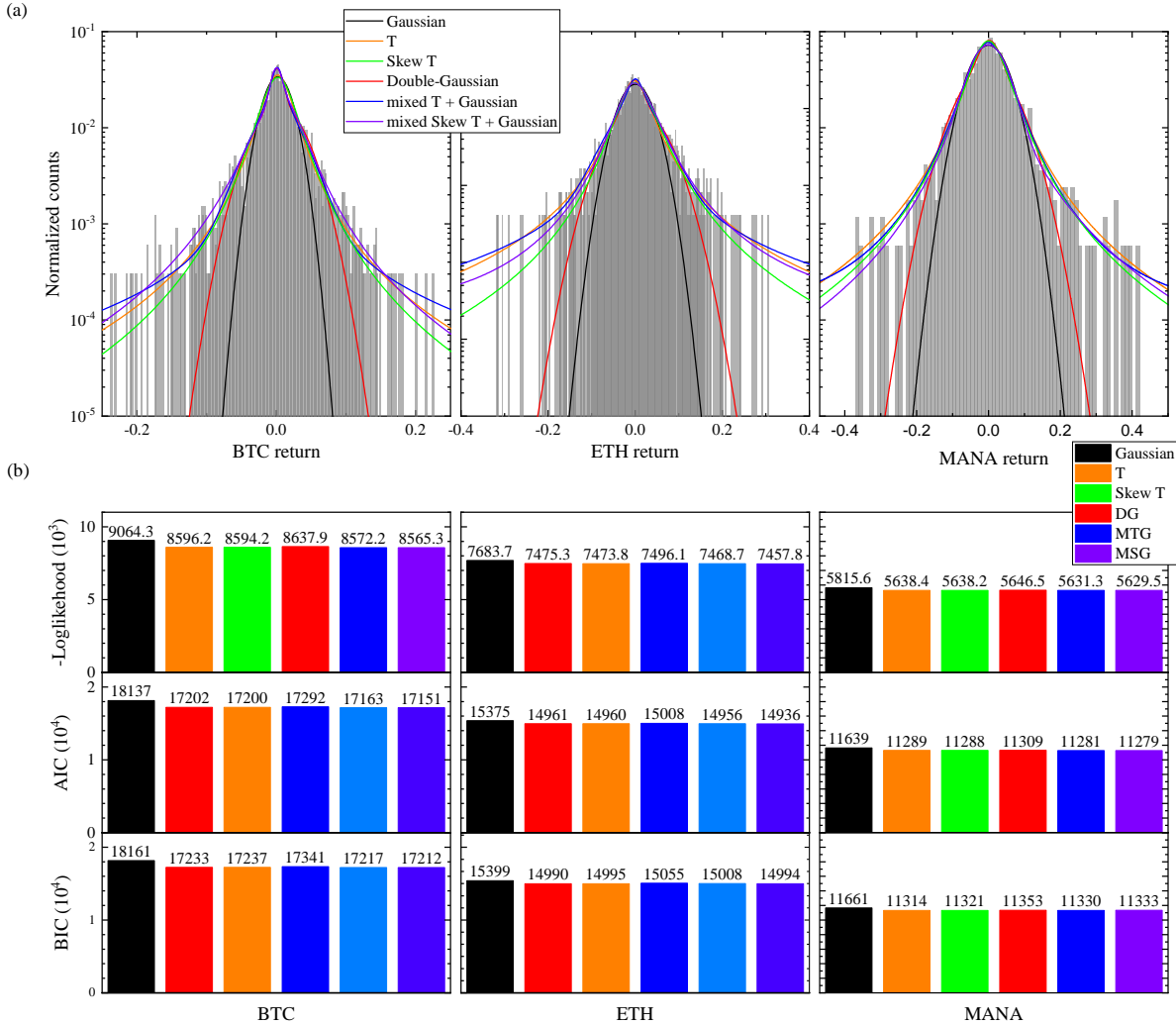


Figure 2: The GARCH(1, 1) model for BTC (Left), ETH (Middle), and MANA (Right) with six distinct PDFs, Namely Gaussian (Black), T (Orange), Skew T (Green), DG (Red), MTG (Blue), and MSG (Purple) distributions. (a) Fitting of the six PDFs to the return distribution. (b) Comparison among three different MLE criteria (AIC, BIC, and Loglikelihood) with the six different PDFs.

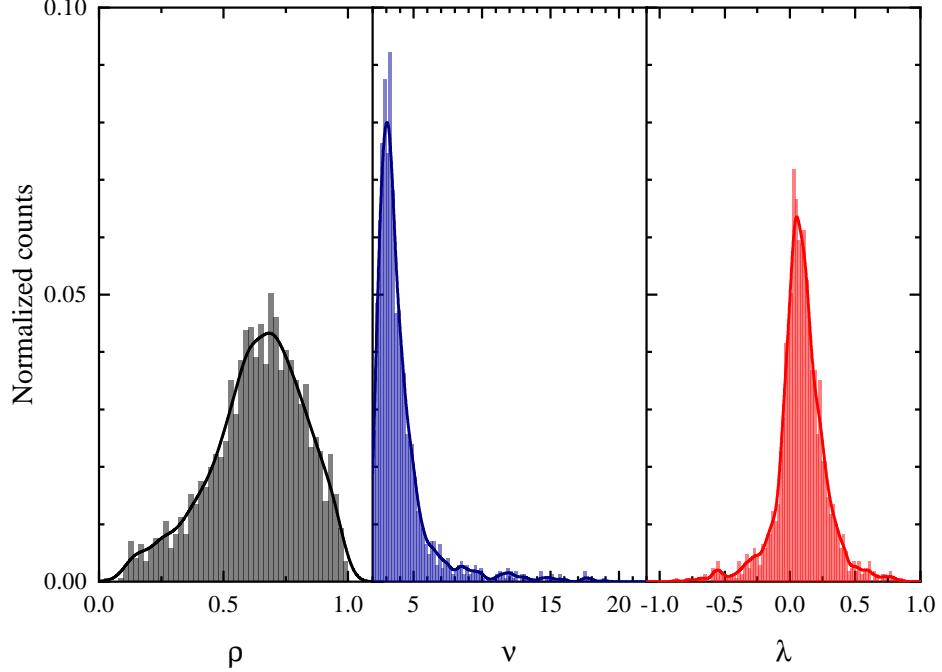


Figure 3: Distribution of the fitted parameters  $\rho$  (left, black),  $\nu$  (middle, blue), and  $\lambda$  (right, red) utilizing the MSG-GARCH model [refer to Eq. (16)] across approximately 3,000 cryptocurrencies.

(BIC) [42], and Log-likelihood ( $\ln(L)$ ). The AIC and BIC are given by:

$$\begin{aligned} \text{AIC} &= -2 \ln(L) + 2N, \\ \text{BIC} &= -2 \ln(L) + N \ln(L), \end{aligned} \tag{18}$$

where  $L$  represents the value of the likelihood function (17) evaluated at the estimated parameters, and  $N$  is the number of parameters estimated. Both the AIC and BIC take into account the precision of the model fit and the number of parameters in the model. These criteria reward a superior fit while penalizing an increased number of parameters in the return series data. The optimal model is identified as the one that minimizes the AIC and BIC values and maximizes the  $\ln(L)$  value.

### 3.3 The Liquidity Risk: VaR<sup>L</sup>

Motivated by the GARCH model and following the suggestion made in [6], we propose a regression model to describe the BAS in the context of a lognormal distribution as per Eq. (5):

$$\begin{aligned} \ln(\text{BAS}_t) &= \mu + \epsilon_t, \\ \sigma_t^2 &= \omega_l + \alpha_l \epsilon_{t-1}^2 + \beta_l \sigma_{t-1}^2. \end{aligned} \tag{19}$$

We employ the MLE method to estimate the parameters  $\omega_l$ ,  $\alpha_l$ ,  $\beta_l$ , and  $\mu$ . The estimated parameters facilitate the prediction of daily liquidity VaR as per Eq. (6) at various confidence levels. We

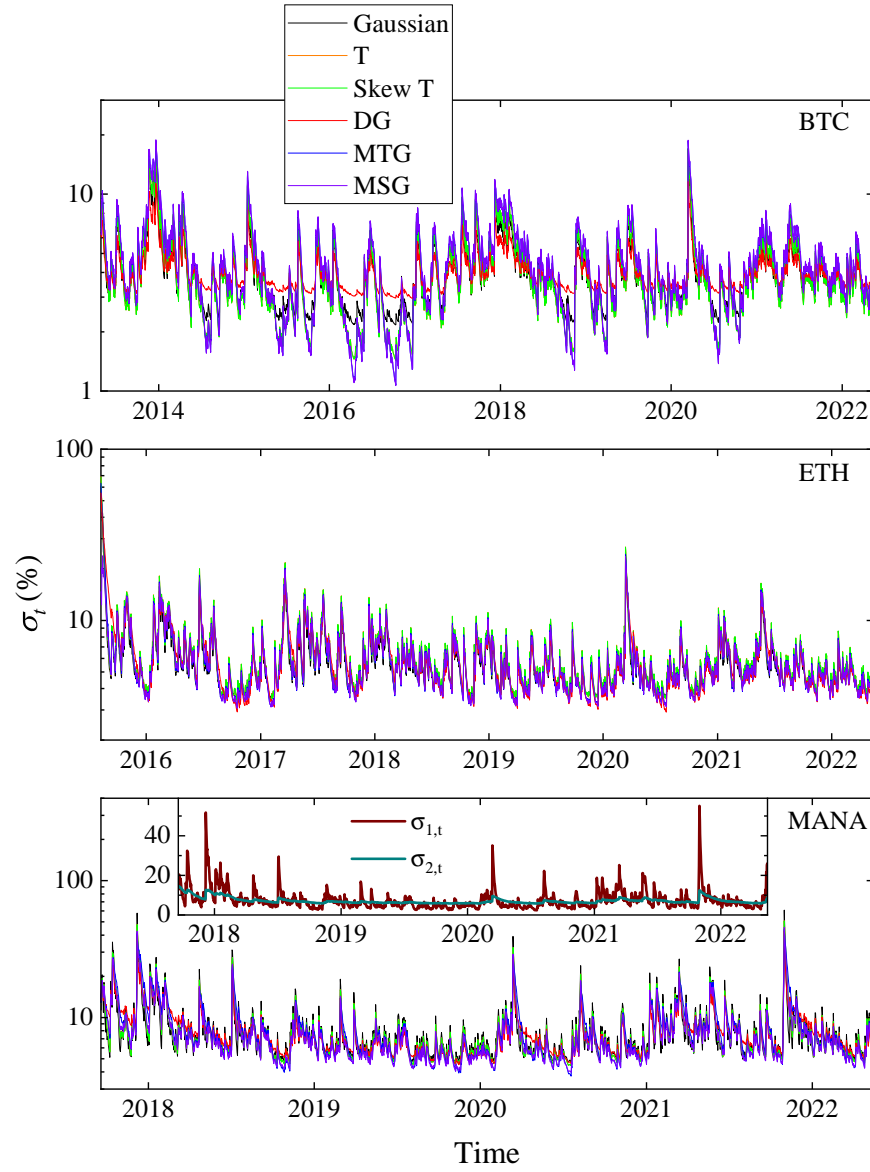


Figure 4: Comparative illustration of volatilities obtained using six distinct PDFs for Bitcoin (BTC; Top), Ethereum (ETH; Middle), and Decentraland (MANA; Bottom). Generally, the MSG-GARCH model predicts a wider range of  $\sigma_t$ . The inset of the bottom figure delineates the two different components of  $\sigma_t$  in the MSG-GARCH model, with  $\sigma_{1,t}$  and  $\sigma_{2,t}$  representing the Skew T and Gaussian components, respectively.

examined different regression models, including a linear term of  $\text{BAS}_t$  in Eq. (19), and found that the above model exhibits superior performance. It is noteworthy to mention that, to the best of our knowledge, such a regression model for estimating liquidity VaR has not been discussed in existing literature. This opens an avenue for future research to explore more sophisticated regression models.

Despite the BAS being most accurately derived from high-frequency data, the practical challenges associated with procuring and processing comprehensive order book data across various cryptocurrency exchanges pose a significant obstacle. Low-frequency measures based on daily transaction data have been explored for cryptocurrencies by [18], suggesting that no single low-frequency measure can be universally optimal. Instead, different measures may prove reasonably effective for varying applications. In this study, we consider two different transaction-based measures to estimate the BAS: the Corwin and Schultz (CS) [43] estimator, and the Abdi and Ranaldo (AR) [44] estimator. These estimators are underpinned by the fundamental concept proposed by Roll [45], suggesting that the transaction price in the market is the sum or difference of the real asset value and the BAS. Consequently, correlations between adjacent daily prices can provide a robust estimate of the BAS. We refrain from considering the original Roll estimator due to its occasional result in irrational correlations that require artificial adjustments [45].

The CS estimator is computed using the high and low prices from two consecutive days as:

$$\text{CS}_{t,t+1} = \frac{2[\exp(a) - 1]}{1 + \exp(a)}, \quad (20)$$

where  $a = \frac{\sqrt{2b}-\sqrt{b}}{3-2\sqrt{2}} - \sqrt{\frac{c}{3-2\sqrt{2}}}$ ,  $b = [\ln(H_t/L_t)]^2 + [\ln(H_{t+1}/L_{t+1})]^2$ , and  $c = [\ln(H_{t,t+1}/L_{t,t+1})]^2$ . Here  $H_t$  ( $L_t$ ) denotes the daily high (low) price, and  $H_{t,t+1}$  ( $L_{t,t+1}$ ) represents the highest (lowest) price across two consecutive days.

The AR estimator, on the other hand, derives the BAS from the natural logarithms of daily high ( $H_t$ ), low ( $L_t$ ), and closing ( $C_t$ ) prices, i.e.  $h_t = \ln(H_t)$ ,  $l_t = \ln(L_t)$ , and  $c_t = \ln(C_t)$ . The AR estimator is defined as follows with  $p_t = (h_t + l_t)/2$ :

$$\text{AR}_t = \sqrt{\max\{4(c_t - p_t)(c_t - p_{t+1}), 0\}} \quad (21)$$

## 4 Results and Discussion

This section presents the empirical findings of the volatility (VaR<sup>V</sup>) and liquidity (VaR<sup>L</sup>) VaR calculations based on the methodology outlined above. We employ GARCH models with diverse distributions to estimate the (VaR<sup>V</sup>). Furthermore, we deduce the LTV, warning, and liquidation ratio for cryptocurrencies based on the computed VaR<sup>V</sup> and VaR<sup>L</sup>. The coins used as examples in

this section are BTC, ETH, and MANA. BTC is the oldest and most recognized cryptocurrency, while ETH and MANA are utilized in Web 3.0 and Metaverse applications, respectively.

## 4.1 GARCH Model Selection and Volatility Estimation

In Fig. 2 (a), we apply the six distinct PDFs discussed in Sec. 3.2.1 to fit the return distributions of BTC (left), ETH (middle), and MANA (right) coins. For all three coins, the best fit is achieved with the MTG or MSG distributions, while the Gaussian and DG distributions provide the poorest fit. These descriptive fittings can serve as indicators when selecting the distribution assumption for the GARCH model, as discussed subsequently.

We now compare the MLE results of GARCH models with different distributions to describe the cryptocurrency volatility. Figure 2 (b) displays examples with data from BTC (left), ETH (middle), and MANA (right), where the three criteria outlined in Sec. 3.2.2 obtained from the MLE method for GARCH models using the six different distributions in Sec. 3.2.1 are plotted (color codes are provided in the figure). The performance of the models varies according to the selected coins. For the BTC data, the use of mixed distributions has significantly improved the description based on all three criteria. For the ETH and MANA data, the Loglikelihood and AIC show improved fitting, but this improvement is not observed for BIC. This indicates that the market dynamics are different for each cryptocurrency, and the most suitable model can be selected to describe the volatility of any given cryptocurrency. After analyzing more than 100 cryptocurrencies, we found that the mixed-distribution (particularly MSG) GARCH model performs the same or better than others in most cases, emphasizing the need for adopting the mixed-distribution assumption. Interestingly, the conclusions drawn from the complex GARCH modeling are consistent with the straightforward descriptive fittings presented in Fig. 2 (a), suggesting the feasibility of using the simple fittings as a rapid selector for distribution assumptions when quick decisions are required.

Table 2 lists all the fitted parameters for different distributions from the MLE method, along with their corresponding fitting errors (indicated in brackets), for BTC, ETH, and MANA. The number of DOF  $\nu$  is fitted to be around  $3 - 4$ , indicating an infinite kurtosis, i.e., the probability is least distributed at the shoulders of the distribution. Small yet significant asymmetries exist in the return distributions of BTC and MANA, as suggested by the corresponding fitted values of  $\lambda$ . The distribution of fitted values of  $\rho$ ,  $\nu$ , and  $\lambda$  for about 3,000 cryptocurrencies applying the MSG-GARCH model is plotted in Fig. 3. The distribution of  $\lambda$  is more skewed towards the positive side, implying positive-skew distributions of returns in the crypto market. This finding aligns with the statistical observation in Fig. 1 (b). Similarly, the distribution of  $\nu$  primarily falls in the range of  $2 - 20$ , indicating the fat-tail effects. This observation corroborates the excess kurtosis calculated in Sec. 2 and Fig. 1 (b). The distribution of  $\rho$  is intriguing as it peaks around 0.7, with very low

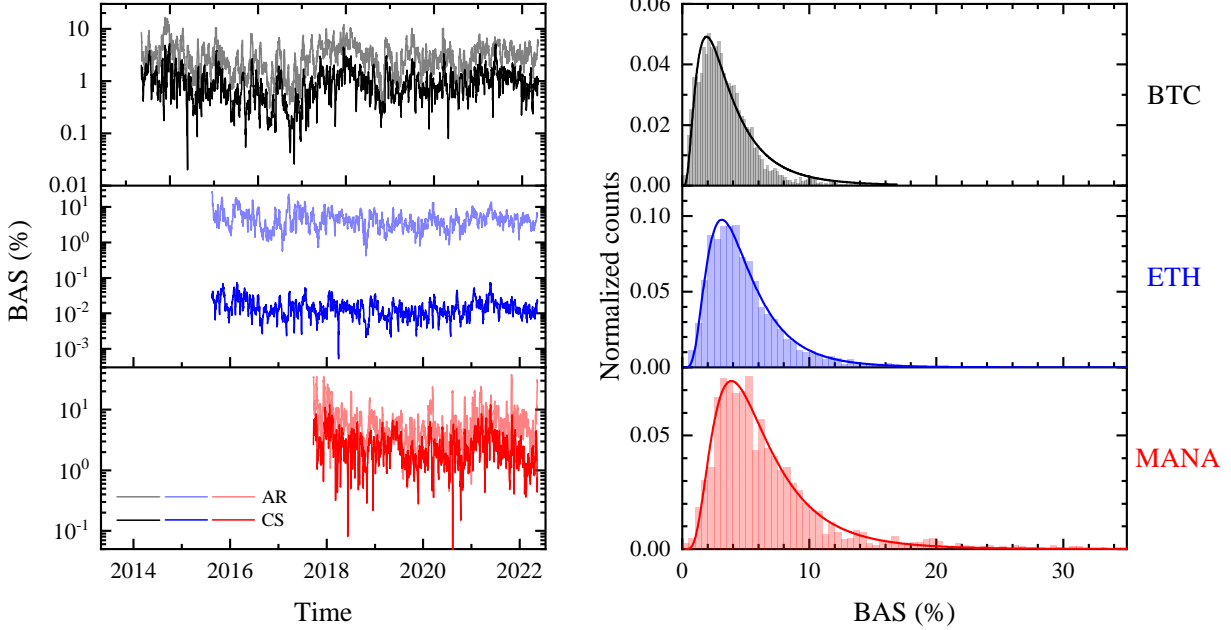


Figure 5: BAS of the BTC, ETH, and MANA coins. On the left, the time-varying AR (light) and CS (dark) estimators of BAS are plotted. On the right, histograms of the AR-estimator data are displayed.

probabilities at 0 or 1, emphatically suggesting the existence of multi-components of return-driving groups in the market. This finding points towards a promising direction for future research on the exploration of the nature of these components.

Utilizing the fitted parameters in Table 2, we estimate the cryptocurrencies’ volatility employing the GARCH process as per Eq. (7) or (10), as depicted in Fig. 4. We set the initial variance for starting the regression using the backcast exponential smoothing method with a parameter of 0.94 [46]. Although the computations of  $\sigma_t$  using different distributions appear relatively similar, they deviate in several instances. The application of mixed dimensions generally results in a wider spread of volatility, as illustrated in Fig. 4 and by the values of  $\beta$  in Table 2 for all three datasets. This suggests stronger volatility clustering effects in the cryptocurrency market. This hypothesis can be tested in future studies.

## 4.2 The bid-ask spread

As outlined in Sec. 3.3, the two BAS estimators are applied to the cryptocurrency data. The results for BTC, ETH, and MANA coins are presented in the left panel of Fig. 5. The AR estimator yields a substantially larger BAS value compared to the CS estimator. Given that large financial institutions typically lean towards a more risk-averse approach and the performance of different

Table 2: MLE Results: Fitted parameters of GARCH model with different distributions introduced in Sec. 3.2.1 for BTC, ETH, and MANA return. The numbers in the brackets indicate the fitting errors in the unit of the last digit of the corresponding fitting value.

Asset	Distribution	Estimated Parameters							
		$\mu_1$	$\mu_2$	$\omega$	$\alpha_1$	$\alpha_2$	$\beta_1$	$\beta_2$	$\rho$
BTC	Gaussian	0.15(6)	-	0.7(3)	0.13(3)	-	0.84(3)	-	-
	T	0.15(4)	-	0.23(14)	0.13(2)	-	0.87(2)	-	3.2(1)
	Skew T	0.10(5)	-	0.23(14)	0.13(2)	-	0.87(2)	-	3.2(1)
	DG	-0.6(4)	0.16(5)	0.02(2)	0.002(5)	0.07(1)	0.999(2)	0.87(2)	-0.04(2)
	MTG	0.09(3)	0.02(9)	0.09(9)	0.17(4)	0.04(3)	0.89(2)	0.5(3)	-
ETH	MSG	0.06(4)	-0.02(9)	0.09(11)	0.18(4)	0.04(3)	0.89(2)	0.48(36)	-0.07(3)
	Gaussian	0.20(10)	-	2.9(8)	0.17(3)	-	0.76(4)	-	-
	T	0.13(7)	-	2.6(6)	0.22(3)	-	0.76(3)	-	3.3(2)
	Skew T	0.22(9)	-	2.6(6)	0.22(3)	-	0.76(3)	-	3.3(2)
	DG	0.3(5)	0.04(11)	1.1(3)	0.22(13)	0.10(2)	0.92(3)	0.72(4)	0.04(2)
MANA	MTG	0.24(8)	-0.75(21)	2.0(5)	0.20(4)	0.06(4)	0.80(3)	0.00(6)	-
	MSG	-0.28(39)	1.29(77)	1.1(5)	0.28(13)	0.03(2)	0.73(4)	0.95(2)	0.78(3)
	Gaussian	-0.02(16)	-	9.8(42)	0.37(12)	-	0.55(13)	-	-
	T	0.03(12)	-	5.3(25)	0.25(8)	-	0.72(9)	-	3.6(3)
	Skew T	0.08(14)	-	5.3(25)	0.25(8)	-	0.72(9)	-	3.6(3)
MANA	DG	1.9(19)	-0.09(11)	2.6(10)	1.0(4)	0.12(3)	0.87(4)	0.75(6)	0.92(8)
	MTG	-0.55(40)	0.73(45)	0.62(54)	0.02(2)	0.42(24)	0.97(3)	0.56(16)	0.60(12)
	MSG	0.65(28)	-1.27(69)	1.2(17)	0.30(6)	0.01(2)	0.72(10)	0.96(4)	0.66(10)
								3.5(4)	0.12(6)

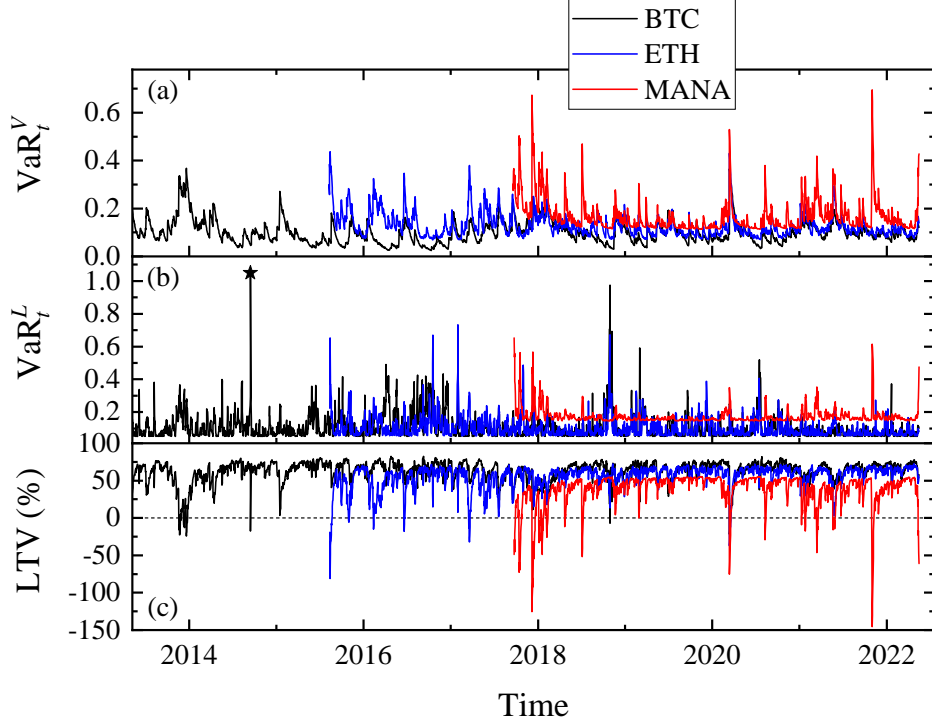


Figure 6: (a) The volatility VaR at 99% C.L. for BTC (Black), ETH (Blue), and MANA (Red) coins. (b) Similar to (a), the Liquidity VaR at 99% C.L. for BTC (Black), ETH (Blue), and MANA (Red) coins. (c) The LTV ratio calculated from the data in (a) and (b) using Eq. (2). Given that we consider a 7-day horizon for LTV, the volatility ( $\sigma$ ) is scaled by a factor of  $\sqrt{7}$  compared with (a).

estimators for cryptocurrencies is yet to be definitively established [18], the AR estimator appears to be the more prudent choice for calculating liquidity VaR. However, it is noteworthy that regardless of the estimator employed, the final  $VaR^L$  is almost identical. This is attributed to the fact that the distributions of logarithmic values from both estimators share similar means and variances [ $\mu$  and  $\sigma^2$  in Eq. (5)], thereby resulting in comparable  $VaR^L$  as per Eq. (6).

As mentioned in Sec. 3.3, the right panel of Fig. 5 displays the BAS distribution employing the AR estimator. The histograms represent the historical data of the three example cryptocurrencies. It is evident that the distributions are not normal and exhibit asymmetry. A lognormal PDF [Eq. (5)] is fitted to the data, and the fitted curves (solid lines in the figure) show excellent agreement with the data points. Consequently, we assume a lognormal distribution of  $BAS_t$  for the regression model in Eq. (19). The parameters obtained from the MLE method are listed in Table 3. For BTC and MANA, a large  $\alpha_l$  (ARCH parameter) and a zero  $\beta_l$  (GARCH parameter) are derived, whereas for ETH, a small  $\alpha_l$  and a large  $\beta_l$  are observed. This trend is further illustrated in Fig. 7, where histograms of fitted  $\alpha_l$  and  $\beta_l$  for approximately 3,000 cryptocurrencies are plotted. The highest probabilities are seen for large  $\alpha_l$  and small  $\beta_l$ , suggesting that the ARCH process is more

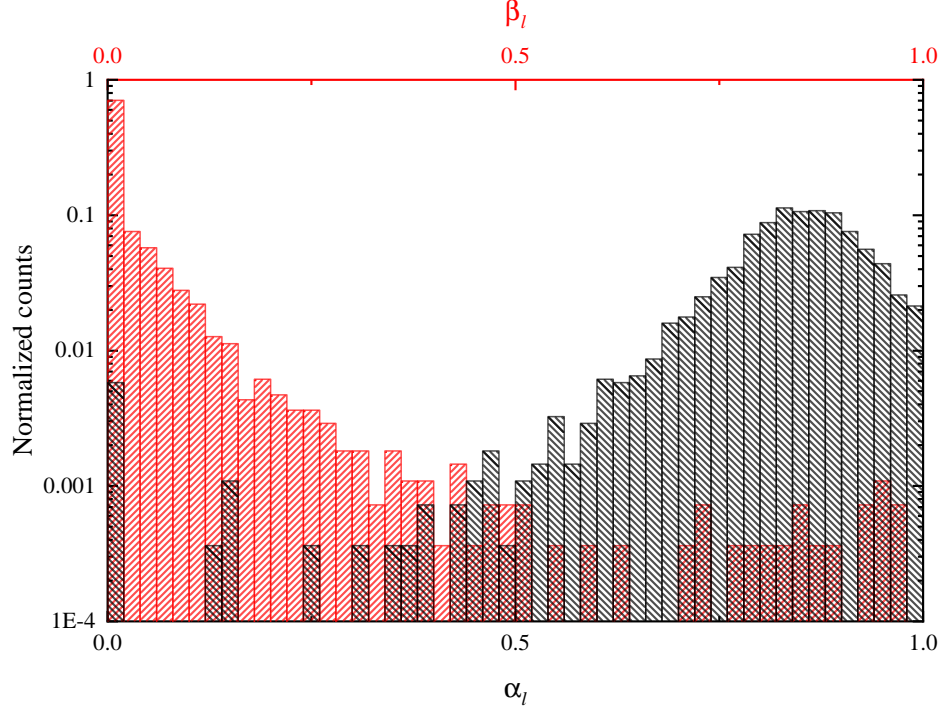


Figure 7: Distribution of the fitted  $\alpha$  (Black) and  $\beta$  (Red) parameters in Eq. (19) for approximately 3,000 cryptocurrencies. The Arch parameter  $\alpha$  predominantly exceeds 0.5, while the GARCH parameter  $\beta$  is generally below 0.5.

prevalent than the GARCH process in the context of BAS volatility.

### 4.3 The volatility and liquidity VaR

In Sec. 4.1, we derived the return volatility, which we subsequently used to compute  $\text{VaR}_t^V$  using Eq. (3). Fig. 7 (a) presents the daily  $\text{VaR}_t^V$  at the 99% confidence level [ $k = 0.01$  in Eq. (3)] for BTC (black curve), ETH (blue curve), and MANA (red curve) coins. This calculation employs the GARCH model with the MSG distribution. To achieve this, we had to numerically derive the inverse function of the CDF for the MSF distribution from Eq. (13). We observe that the returns for BTC and ETH become less volatile as they mature, whereas the MANA coin continues to exhibit significant fluctuations, indicative of its relative immaturity. Furthermore, MANA presents a higher average and maximum  $\text{VaR}_t^V$  than BTC and ETH, which aligns with expectations.

We calculate  $\text{VaR}_t^L$  using Eq. 6, with  $\mu$  and  $\sigma$  obtained from the regression model in Eq. (19). The results for BTC, ETH, and MANA are depicted in Fig. 6 (b). Similar to the volatility risk  $\text{VaR}_t^V$ , the average liquidity risk for ETH is marginally higher than that of BTC, with both being significantly smaller than the MANA value. Interestingly, we observe sharp spikes in the  $\text{VaR}_t^L$  plot for BTC and ETH, which are not present in the corresponding  $\text{VaR}_t^V$  plot. For instance, the highest peak

Table 3: MLE results: fitted parameters of the regression model Eq. (19) to describe the BAS distribution for BTC, ETH, and MANA. The numbers in brackets indicate the fitting errors in the unit of the last digit of the corresponding fitting value.

	Asset	BTC	ETH	MANA
<b>Parameters</b>	$\mu$	-3.49(2)	-3.16(3)	-2.89(2)
	$\omega_l$	0.074(7)	0.077(8)	0.08(1)
	$\alpha_l$	0.88(4)	0.82(6)	0.82(5)
	$\beta_l$	0.00(3)	0.00(5)	0.00(4)
<b>Criteria</b>	$\ln(L)$	-2670.3	-1815.6	-1225.2
	AIC	5349	3639	2458
	BIC	5373	3662	2480

for BTC on 2014-09-15, denoted by the star. These spikes could stem from model imperfections or real effects such as temporary large liquidity costs, warranting case-by-case investigation.

The Pearson correlation coefficients between  $\text{VaR}_t^V$  and  $\text{VaR}_t^L$  in Figs. 6 (a) and 6 (b) are -0.11, 0.20, and 0.83 for BTC, ETH, and MANA, respectively. A positive correlation between  $\text{VaR}_t^V$  and  $\text{VaR}_t^L$  suggests that increased price volatility corresponds to reduced market liquidity, and vice versa for a negative correlation. A positive correlation, such as with ETH and MANA data, aligns with our intuition [35], while a negative correlation, as observed in the BTC data, is unexpected and counter-intuitive.

#### 4.4 LTV, Warning, and Liquidation Ratios

The VaR computed in Sec. 4.3 is daily, enabling the prediction of VaR within a certain time horizon, encapsulating both volatility and liquidity risks, as per Eqs. (7) [or Eq. (10)] and (19). In the context of a collateral loan, when examining the LTV, warning, and liquidation ratios, the complementary part of VaR, denoted as Eq. (2), is considered safe, thereby establishing these ratios. Moreover, risks are typically associated with a specified time horizon, and the longer this horizon, the greater the risks. Therefore, in this study, we compute the LTV, warning, and liquidation ratios using Eq. (2) over time horizons of seven, three, and one day, respectively.

Fig. 6 (c) illustrates the calculated LTV ratio utilizing  $\text{VaR}_t^V$  and  $\text{VaR}_t^L$  from Figs. 6 (a) and 6 (b), respectively. The volatility scales with the time horizon  $T$  as  $\sigma_T \propto \sqrt{T}$ . As expected, higher LTV ratios can be secured for BTC and ETH, whereas MANA yields a smaller LTV value. It is important to note that downside peaks in the calculated LTV ratios can reach negative values, corresponding to either historical price crises or spikes identified in the liquidity VaR plot in Fig. 6 (b). In Table 4, we present the average LTV, warning, and liquidation ratios derived from his-

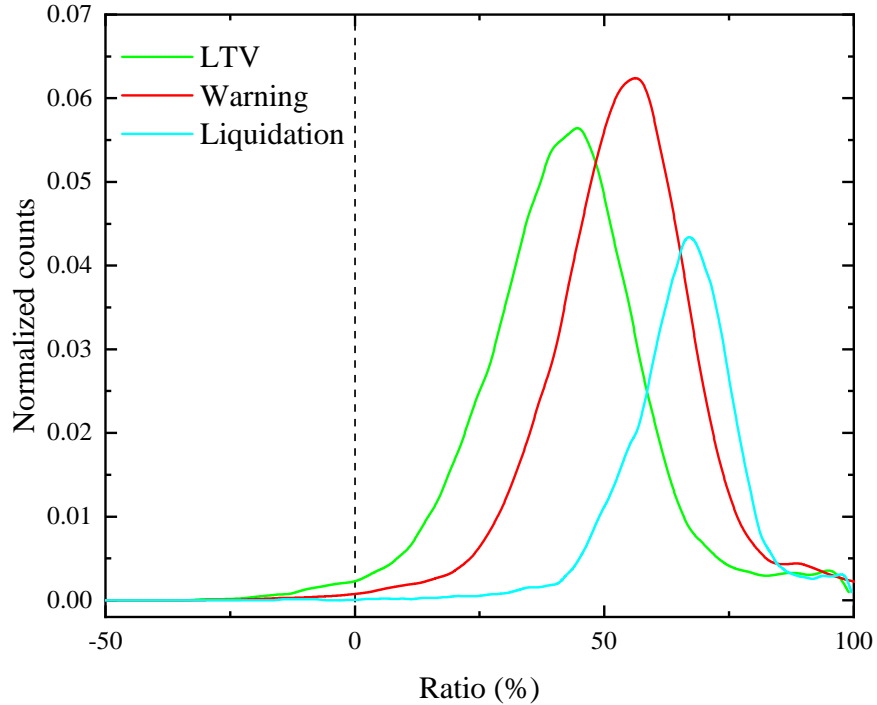


Figure 8: Distributions of the LTV (green), warning (red), and liquidation (cyan) ratios for approximately 3,000 cryptocurrencies.

torical data for the top 10 cryptocurrencies by market capitalization. These can be compared with corresponding figures from existing platforms, as shown in Table 1. The LTV ratio ranges from approximately 50% to 70%, aligning with most existing collateral loan products available in the market (see Table 1), and similarly for warning and liquidation ratios.

We calculate the LTV, warning, and liquidation ratios for all top 3,000 cryptocurrencies, the distributions of which are depicted in Fig. 8. Over 70% of cryptocurrencies have an LTV ratio of less than 50%, with a few demonstrating negative values. Our data enable the design of various types of cryptocurrency collateral loans. For instance, lenders may allow only specific cryptocurrencies with an LTV exceeding a desired threshold to qualify as collateral. Alternatively, consideration may be given to constructing portfolios of cryptocurrencies, which would necessitate the development of further models incorporating correlations among different cryptocurrencies.

## 4.5 Back Test

During the final stages of this study, two periods of significant market downturns were observed in the cryptocurrency market, as illustrated in Fig. 9 (a). For "Period 1" and "Period 2", price data from 2022-05-03 to 2022-06-06 and 2022-06-09 to 2022-07-08, respectively, was used, with data intervals set at a minute. This data was sourced from the centralized exchange, Binance. The prices

Table 4: LTV, warning, liquidation ratios for the top 10 cryptocurrencies.

Crypto	LTV (%)	Warning(%)	Liquidation(%)
BTC	69	76	83
ETH	62	71	79
BNB	59	69	77
XRP	61	70	78
ADA	56	66	76
SOL	51	63	73
DOGE	53	63	73
DOT	59	69	78
WBTC	72	79	85
AVAX	50	62	72

of nine cryptocurrencies (excluding WBTC), listed in Table 4, were plotted. During both periods, all of these cryptocurrencies experienced substantial price drops, ranging between 30–50%. These periods provide ideal opportunities to back-test our collateral loan calculations.

The back-testing process commenced by employing the calculated LTV ratios from Table 4 as the initial LTV (also known as the healthy ratio) for each of the nine cryptocurrencies. The total loan amount was fixed [US\$30 million in Fig. 9 (b)]. The LTV ratio was re-evaluated every minute as the cryptocurrency price evolved. A warning would be issued once the LTV reached the warning ratio (as per Table 4), lasting until the LTV returned to a healthy value due to either additional collateral being supplied by borrowers or the cryptocurrency price rebounding. Liquidation would be triggered when the liquidation threshold was hit, or a warning persisted for more than three days, and it would not cease until the LTV returned to the healthy value.

To refine our back-testing model, collateral was liquidated at one-minute intervals at a volume of 1% of the last-minute market trading volume, thereby minimizing the price impact of our liquidation process. The LTV ratio was subsequently recalculated as follows:

$$\text{LTV}_{i+1} = \frac{T_i - 0.01V_{i-1}C_i}{(L_i - 0.01V_{i-1})C_i}, \quad (22)$$

where  $T_i$ ,  $C_i$ ,  $V_i$ , and  $L_i$  denote the remaining loan, price, market volume, and remaining position at the  $i$ th minute, respectively, with  $T_0$  as the initial loan amount and  $L_0 = T_0/C_0$ . The calculated LTVs (blue curves) are presented in Fig. 9 (b), demonstrating the performance of collateral loans with the nine selected cryptocurrencies throughout the two back-testing periods. For comparison, we also display the LTVs in the absence of liquidation (black curves). In all scenarios, our liquidation strategy successfully reduces the LTV back to a healthy value (indicated by the green dotted line), demonstrating the riskiness of the loans should no actions be undertaken.

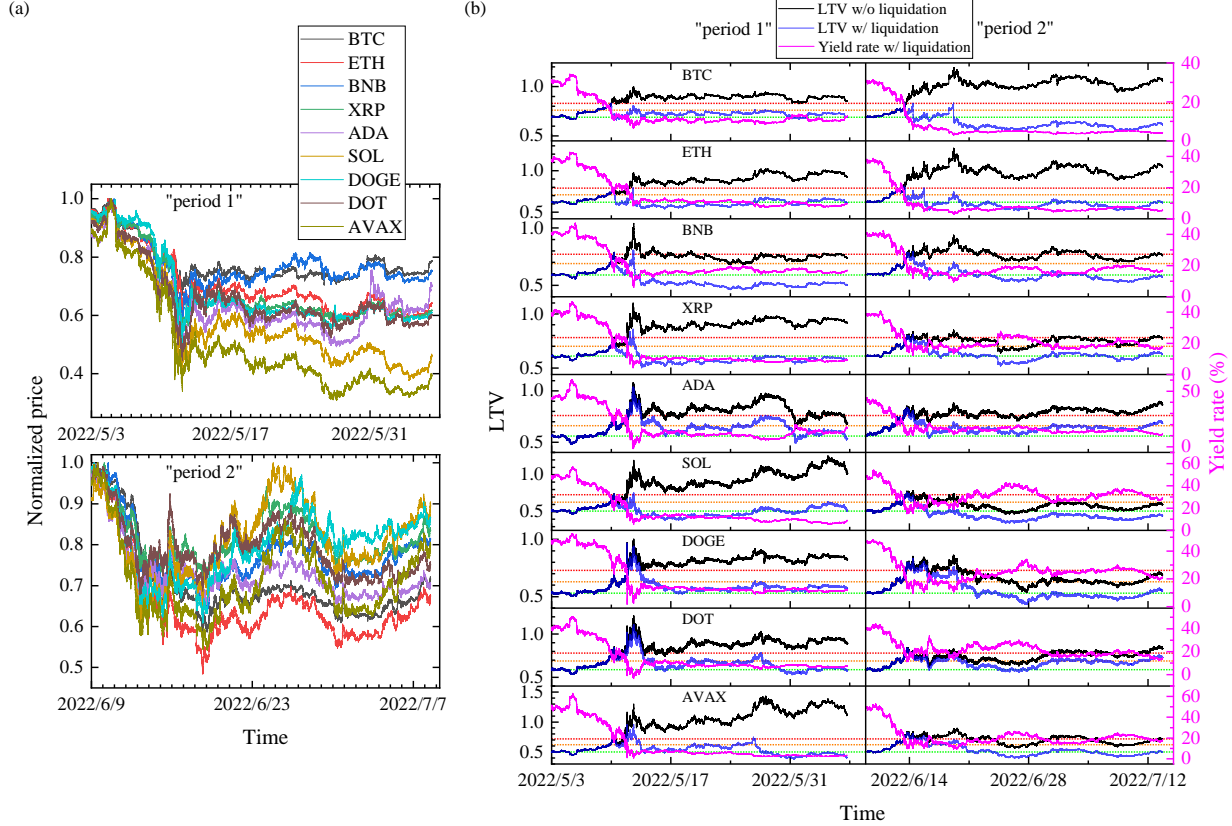


Figure 9: Backtesting cryptocurrency-backed loans. (a) Normalized price of 9 cryptocurrencies (see Table 4) excluding WBTC) during two time windows: "Period 1" is from 2022-05-03 to 2022-06-06 and "Period 2" is from 2022-06-09 to 2022-07-08. All quoted cryptocurrencies experience a crash, with the worst losses reaching approximately 70%. (b) Monitored LTV with (black curves) and without (blue curves) the liquidation process and the corresponding yield rate in Eq. (23) during the two periods in (a). In all instances, our liquidation strategy contributes to maintaining the health of the loans. Losses are avoided, except ADA and DOT coins within a very brief period in "period 1" (approximately half a day), where a maximum loss of around 3.5% is observed. For this analysis, we assume a loan amount of US\$ 30 million and no delay time.

To ascertain the occurrence of severe losses, we define the yield rate as:

$$lr_i = \left(1 - \frac{T_i}{T_0}\right)(1 - \rho) + \frac{L_i C_i}{T_0} - 1, \quad (23)$$

where  $\rho$  represents the ratio of trading fees charged by exchanges. The yield rate resulting from liquidation during both periods is displayed in Fig. 9 (b), where we mostly observe  $lr_i > 0$  with a maximum loss of approximately 3.5% for the DOT coin within half a day. No significant losses are observed in all cases.

Two practical factors can significantly influence the liquidation behavior, notably affecting the LTV in Eq. 22 and the yield rate in Eq. 23. These are the liquidation delay and the total loan amount. A delay can occur when liquidation is triggered due to operational requirements or a chosen liquidation strategy. In Fig. 10 (a), we examine the effects of varying liquidation delays, from no delay to a delay of three days, on the back-testing result of the DOT coin. This coin exhibited the largest losses in Fig. 9 (b). LTV behaviors vary under different liquidation delays, while yield rates appear relatively insensitive to them. This may be attributed to the fact that the cryptocurrency market not only experiences significant crashes but also rapid recoveries, rendering the liquidation delay less important compared to markets with protracted recovery phases.

The loan amount,  $T_0$ , plays a pivotal role in the current liquidation scheme, given that the liquidation process is heavily dependent on the market trading volume. As illustrated in Fig. 10 (b), for a smaller loan amount, either liquidation is swiftly and easily executed (denoted by a LTV  $\gg 1$ , black curve), or the loan is promptly repaid (denoted by a negative LTV, red curve). In both instances, a constant yield rate is achieved post-liquidation. However, the yield rate diminishes for larger loan amounts during a crash, and the LTV behavior with a substantial loan amount is strongly reliant on market dynamics since the trading volume is insufficient to absorb all collateral intended for liquidation.

## 5 Conclusion and Outlook

We devised a robust procedure to compute the LTV, warning, and liquidation ratios for cryptocurrencies considered as collateral for loans. These computed LTV, warning, and liquidation ratios have been tested during two recent crash periods in the cryptocurrency market, and have demonstrated their effectiveness as a safeguard for crypto collateral loans.

Our model considers both volatility and liquidity risks within the VaR framework. For volatility risk, we have evaluated six different distributions for the return residual within the standard GARCH model, revealing that mixed distributions frequently deliver the best performance. Future research will delve deeper into attributing components of volatility to distinct groups of market

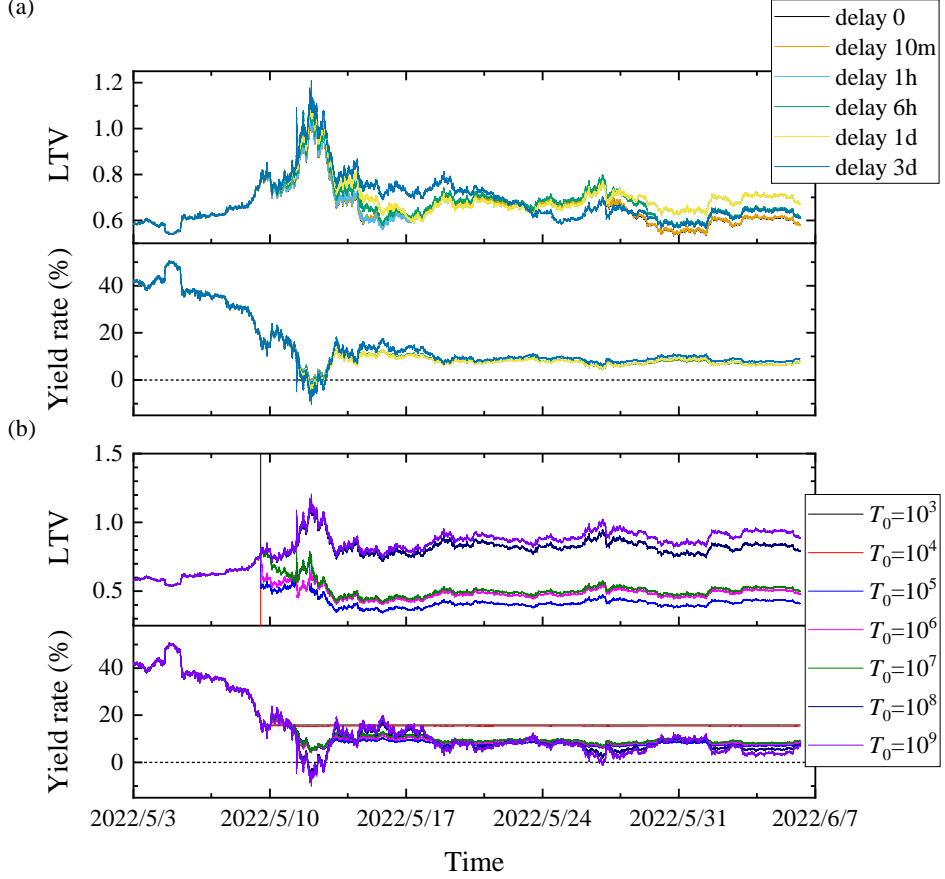


Figure 10: Effects of delay and loan amount on liquidation of crypto collateral loans. (a) LTV and yield rate with different delays for the DOT coin. While LTVs are affected by liquidation delay, the loss rates remain relatively stable. (b) LTV and yield rate with loan amounts ( $T_0$ ) for the DOT coin. The loan amount exerts a substantial impact on both LTV and yield rate, owing to its interaction with the market volume in our liquidation scheme.

participants. Concerning liquidity risk, we have developed a regression model that describes and predicts the liquidity VaR, premised on the assumption that the risk measure, BAS, follows a log-normal distribution.

Some unresolved questions include understanding how to incorporate horizon-dependent liquidity risk and comprehending the correlations between volatility and liquidity within the cryptocurrency market. With the above quantitative tools developed, we hope to stimulate more investigations into similar financing and banking models along with the rise of the crypto market, like NFT-based collateral loans.

## References

- [1] K. Malinova, A. Park, Tokenomics: when tokens beat equity, *Management Science* 0 (0) (2023).
- [2] A. N. Berger, G. F. Udell, Collateral, loan quality and bank risk, *Journal of Monetary Economics* 25 (1) (1990) 21–42.
- [3] R. J. Barro, The loan market, collateral, and rates of interest, *Journal of Money, Credit and Banking* 8 (4) (1976) 439–456.
- [4] N. Cai, W. Zhang, Regime classification and stock loan valuation, *Operations Research* 68 (4) (2020) 965–983.
- [5] Y. Jiang, Y.-C. Ho, X. Yan, Y. Tan, When online lending meets real estate: Examining investment decisions in lending-based real estate crowdfunding, *Information Systems Research* 31 (3) (2020) 715–730.
- [6] A. Bangia, F. X. Diebold, T. Schuermann, J. Stroughair, Modeling liquidity risk with implications for traditional market risk measurement and management, *SSRN* (2008).
- [7] R. Tsaih, Y.-J. Liu, W. Liu, Y.-L. Lien, Credit scoring system for small business loans, *Decision Support Systems* 38 (1) (2004) 91–99.
- [8] P. Jorion, Risk2: Measuring the risk in value at risk, *Financial analysts journal* 52 (6) (1996) 47–56.
- [9] L. Guan, A. Abbasi, M. J. Ryan, A simulation-based risk interdependency network model for project risk assessment, *Decision Support Systems* 148 (2021) 113602.
- [10] T. Bollerslev, Generalized autoregressive conditional heteroskedasticity, *Journal of Econometrics* 31 (3) (1986) 307–327. doi:10.1016/0304-4076(86)90063-1.
- [11] T. J. Linsmeier, N. D. Pearson, Value at risk, *Financial analysts journal* 56 (2) (2000) 47–67.
- [12] F. Caron, J. Vanthienen, B. Baesens, Comprehensive rule-based compliance checking and risk management with process mining, *Decision Support Systems* 54 (3) (2013) 1357–1369.
- [13] C. N. Kim, H. M. Chung, D. B. Paradice, Inductive modeling of expert decision making in loan evaluation: a decision strategy perspective, *Decision Support Systems* 21 (2) (1997) 83–98.
- [14] S. Y. Chun, M. A. Lejeune, Risk-based loan pricing: Portfolio optimization approach with marginal risk contribution, *Management Science* 66 (8) (2020) 3735–3753.
- [15] S. Frühwirth-Schnatter, G. Celeux, C. P. Robert (Eds.), *Handbook of Mixture Analysis*, CRC Press, Taylor & Francis Group, 2019.
- [16] M. Haas, Mixed Normal Conditional Heteroskedasticity, *Journal of Financial Econometrics* 2 (2) (2004) 211–250. doi:10.1093/jjfinec/nbh009.

- [17] D. Ryu, R. I. Webb, J. Yu, Liquidity-adjusted value-at-risk: a comprehensive extension with microstructural liquidity components, *The European Journal of Finance* 28 (9) (2022) 871–888.
- [18] A. Brauneis, R. Mestel, R. Riordan, E. Theissen, How to measure the liquidity of cryptocurrency markets?, *Journal of Banking & Finance* 124 (2021) 106041. doi:<https://doi.org/10.1016/j.jbankfin.2020.106041>.
- [19] H. Guo, D. Zhang, S. Liu, L. Wang, Y. Ding, Bitcoin price forecasting: A perspective of underlying blockchain transactions, *Decision Support Systems* 151 (2021) 113650.
- [20] C. Zhong, W. Du, W. Xu, Q. Huang, Y. Zhao, M. Wang, LSTM-ReGAT: A network-centric approach for cryptocurrency price trend prediction, *Decision Support Systems* 169 (2023) 113955.
- [21] X. Li, C. A. Wang, The technology and economic determinants of cryptocurrency exchange rates: The case of bitcoin, *Decision support systems* 95 (2017) 49–60.
- [22] J. Chod, E. Lyandres, A Theory of ICOs: Diversification, Agency, and Information Asymmetry, *Management Science* 67 (10) (2021) 5969–5989. doi:[10.1287/mnsc.2020.3754](https://doi.org/10.1287/mnsc.2020.3754).
- [23] J. R. Gan, G. Tsoukalas, S. Netessine, Initial Coin Offerings, Speculation, and Asset Tokenization, *Management Science* 67 (2) (2021) 914–931. doi:[10.1287/mnsc.2020.3796](https://doi.org/10.1287/mnsc.2020.3796).
- [24] J. R. Gan, G. Tsoukalas, S. Netessine, Decentralized Platforms: Governance, Tokenomics, and ICO Design, *Management Science* (2023) mnsc.2021.02076 doi:[10.1287/mnsc.2021.02076](https://doi.org/10.1287/mnsc.2021.02076).
- [25] S. Y. Jin, Z. T. Li, A. Huang, K. Y. Tam, Token-based platforms and green dilemma: Examining the role of community perceptions and web page environmental disclosures, Available at SSRN 4569995 (2023).
- [26] O. Lavastre, A. Gunasekaran, A. Spalanzani, Supply chain risk management in french companies, *Decision Support Systems* 52 (4) (2012) 828–838.
- [27] D. Slof, F. Frasincar, V. Matsiiako, A competing risks model based on latent dirichlet allocation for predicting churn reasons, *Decision Support Systems* 146 (2021) 113541.
- [28] H.-J. Li, X.-G. Luo, Z.-L. Zhang, W. Jiang, S.-W. Huang, Driving risk prevention in usage-based insurance services based on interpretable machine learning and telematics data, *Decision Support Systems* (2023) 113985.
- [29] J. Xiao, Z. Wen, X. Jiang, L. Yu, S. Wang, Three-stage research framework to assess and predict the financial risk of smes based on hybrid method, *Decision Support Systems* (2023) 114090.
- [30] Z. Yi, Z. Liang, T. Xie, F. Li, Financial risk prediction in supply chain finance based on buyer transaction behavior, *Decision Support Systems* 170 (2023) 113964.
- [31] P. Saha, I. Bose, A. Mahanti, A knowledge based scheme for risk assessment in loan processing by banks, *Decision Support Systems* 84 (2016) 78–88.

- [32] J. R. Booth, L. C. Booth, Loan collateral decisions and corporate borrowing costs, *Journal of Money, Credit and Banking* 38 (1) (2006) 67–90.
- [33] R. Cont, Empirical properties of asset returns: stylized facts and statistical issues, *Quantitative Finance* 1 (2) (2001) 223.
- [34] C. Francq, J.-M. Zakoian, GARCH models: structure, statistical inference and financial applications, John Wiley & Sons, 2019.
- [35] M. Wyart, J.-P. Bouchaud, J. Kockelkoren, M. Potters, M. Vettorazzo, Relation between bid–ask spread, impact and volatility in order-driven markets, *Quantitative Finance* 8 (1) (2008) 41–57.
- [36] G. Petrella, R. Segara, The bid–ask spread of bank-issued options: A quantile regression analysis, *Quantitative Finance* 13 (8) (2013) 1241–1255. doi:10.1080/14697688.2012.728006.
- [37] L. Feng, Y. Shi, A simulation study on the distributions of disturbances in the garch model, *Cogent Economics and Finance* 5 (1) (2017) 1–19.
- [38] M. Orhan, B. Köksal, A comparison of garch models for var estimation, *Expert Systems with Applications* 39 (3) (2012) 3582–3592.
- [39] P. Katsiampa, Volatility estimation for Bitcoin: A comparison of GARCH models, *Economics Letters* 158 (2017) 3–6. doi:10.1016/j.econlet.2017.06.023.
- [40] S. A. Gyamerah, Modelling the volatility of bitcoin returns using garch models, *Quantitative Finance and Economics* 3 (4) (2019) 739–753.
- [41] C. S. Wong, W. K. Li, On a Mixture Autoregressive Conditional Heteroscedastic Model, *Journal of the American Statistical Association* 96 (455) (2001) 982–995. doi:10.1198/016214501753208645.
- [42] G. Schwarz, Estimating the dimension of a model, *The Annals of Statistics* 6 (2) (1978) 461–464.
- [43] S. A. Corwin, P. Schultz, A Simple Way to Estimate Bid-Ask Spreads from Daily High and Low Prices, *The Journal of Finance* 67 (2) (2012) 719–760. doi:10.1111/j.1540-6261.2012.01729.x.
- [44] F. Abdi, A. Ranaldo, A Simple Estimation of Bid-Ask Spreads from Daily Close, High, and Low Prices, *The Review of Financial Studies* 30 (12) (2017) 4437–4480. doi:10.1093/rfs/hhx084.
- [45] R. Roll, A Simple Implicit Measure of the Effective Bid-Ask Spread in an Efficient Market, *The Journal of Finance* 39 (4) (1984) 1127–1139. doi:10.1111/j.1540-6261.1984.tb03897.x.
- [46] G. Sbrana, A. Silvestrini, Aggregation of exponential smoothing processes with an application to portfolio risk evaluation, *Journal of Banking & Finance* 37 (5) (2013) 1437–1450.